

ON THE USE OF HIGHER ORDER STATISTICS IN SAS IMAGERY

F. Maussang, J. Chanussot

Laboratoire des Images et des Signaux – CNRS
LIS / ENSIEG – Domaine Universitaire – BP 46
38402 Saint-Martin-d’Hères Cedex, France
{frederic.maussang; jocelyn.chanussot}@lis.inpg.fr

A. Hézet

Groupe d’Etudes Sous-Marines de l’Atlantique
DGA/DCE/GESMA – BP 42
29240 Brest Naval, France
hetet@gesma.fr

ABSTRACT

Synthetic Aperture Sonar (SAS) imagery is largely used in detection, location and classification of underwater mines laying or buried in the sea bed. This paper proposes a detection method using Higher Order Statistics (HOS) on SAS images. The proposed method can be divided into two steps. Firstly, the HOS (Skewness and Kurtosis) are locally estimated using a square sliding computation window. In a second step, the results are focused by a correlation process. This enables the precise location of the objects. This method is tested on real SAS data containing both underwater mines laying on the sea bed and buried objects.

1. INTRODUCTION

The detection and classification of different types of underwater mines is a present crucial strategic task [1]. Thanks to their high resolution, the images provided by Synthetic Aperture Sonar (SAS) are of great interest for this purpose and have been increasingly used in sea bed imagery. After a classical processing, the beam-forming, interesting information can be extracted from SAS images of the sea bed.

But these images are seriously corrupted by a speckle noise which gives a granular aspect to the image and disturbs its interpretation. A plentiful literature deals with processing of sonar images to enhance information. Some of the methods use smoothing filters [2]. Other papers propose segmentation methods [3, 4] based on a statistical model or using first and second order statistics. Higher Order Statistics (HOS) have been used as a powerful tool in various signal processing applications [5, 6]. Nevertheless, they have very rarely been used to address sonar applications. To our knowledge, the only example is given by *Aridgides et al.* [7] who used HOS estimators (Skewness and Kurtosis) to extract features from side scan sonar images in order to classify sea mines by a fusion process.

In this paper, a detection method using third and fourth order statistics is proposed. It can be divided into two steps. In the first step, Kurtosis and Skewness are evaluated on a square window for each pixel of the image (section 2). The second step consists in focusing the result in order to obtain the correct location of the detected object (section 3). Finally, this method is tested on real data containing both underwater mines laying on the sea bed and buried objects (section 4).

2. HOS ESTIMATORS ON SAS IMAGES

2.1. Definition of the estimators

Among the plentiful choice of tools proposed by the Higher Order Statistics (HOS), the most famous estimators are Skewness (3rd order moment) and Kurtosis (4th order) [8]. If the r th order central moment of random samples X is noted $\mu_{X(r)}$, the definition of the Skewness estimated on X is given by:

$$\mathcal{S}_X = \frac{\mu_{X(3)}}{\mu_{X(2)}^{3/2}} \quad (1)$$

A definition of the Kurtosis is given by:

$$\mathcal{K}_X = \frac{\mu_{X(4)}}{\mu_{X(2)}^2} - 3 \quad (2)$$

Skewness gives a measure of symmetry of a random distribution, and Kurtosis measures whether the data are peaked or flat relative to a normal distribution. These estimators are null for a normal distribution.

2.2. Results on a synthetic image

To introduce the detection method used in this paper, it is tested on a synthetic image modelling a SAS image. It consists of a square (11×11) (Fig. 1), with an amplitude of 10, modeling the echo reflected by an object, surrounded by a noise. A Weibull law describes efficiently the amplitude R of the noise in a SAS image [4]. Therefore, the noise on the synthetic image is generated by a Weibull law described by the following probability density function:

$$\mathcal{W}_R(R) = \frac{\delta}{\alpha} \left(\frac{R}{\alpha}\right)^{\delta-1} \exp\left\{-\left(\frac{R}{\alpha}\right)^\delta\right\}; R \geq 0 \quad (3)$$

with $\alpha = 0.25$ (this ensures a realistic signal to noise ratio) and $\delta = 1.65$ (this value being estimated close to the parameter on real data).

Skewness and Kurtosis are then evaluated on a square window (11×11 here) for each pixel of the image (Fig. 2). The choice of the size of the estimation window is discussed in the next subsection.

To explain the results obtained on Fig. 2, we consider p the proportion of the filtering window composed of deterministic pixels (i.e. belonging to the simulated echo) and $(1 - p)$ the proportion of random values (Fig. 1). Considering $\mu'_{E(r)}$, $\mu'_{N(r)}$ and

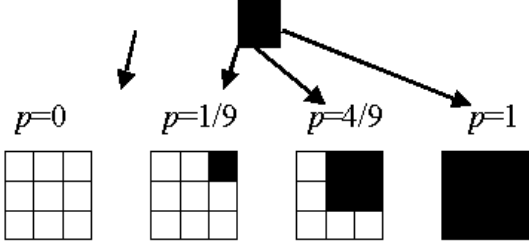


Fig. 1. Modelised echo and definition of the parameter p .

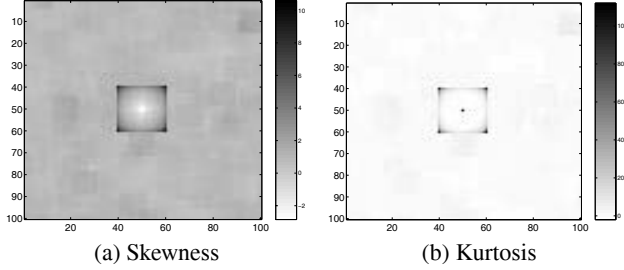


Fig. 2. Skewness and Kurtosis evaluated on the synthetic image with a 11×11 window.

$\mu'_{X(r)}$ the r th order non-central moments respectively computed on the “echo-part” of the filtering window, the “noise-part”, and the whole window, the following relation holds:

$$\mu'_{X(r)} = p \cdot \mu'_{E(r)} + (1 - p) \cdot \mu'_{N(r)} \quad (4)$$

Moreover, considering A the amplitude of the echo and the Weibull law describing the noise (equation 3), we have:

$$\mu'_{E(r)} = A^r \quad \text{and} \quad \mu'_{N(r)} = \alpha^r \Gamma(1 - r/\delta) \quad (5)$$

If the moments of the noise are supposed to be negligible compared with the moments of the echo, and if we take into account the relationship between the central and non-central moments [8], an approximation of Skewness (equation 1) can be made by:

$$\mathcal{S}_X(p) \approx \frac{1 - 3p + 2p^2}{p^{1/2}(1 - p)^{3/2}} \quad (6)$$

Similarly, an approximation of Kurtosis (equation 2) is given by:

$$\mathcal{K}_X(p) \approx \frac{1 - 7p + 12p^2 - 6p^3}{p(1 - p)^2} \quad (7)$$

The behaviour of these approximations versus parameter p is shown on Fig. 3. An interesting property is the independence of these values from the amplitude of the echo.

From the results presented on Fig. 2, we can make the following observations:

- In the noisy background, the HOS estimators lead to small values. This corresponds to the low values of the statistical moments of the Weibull law (note that in this specific case, the approximations proposed in (6) and (7) do not hold anymore).
- Square structures can be seen around the echo. They are composed of pixels with high values, the highest being in the corners.

The size of these squares corresponds to the size of the echo (11) plus the size of the computation window (11). As can be seen on Fig. 3, the maximal values for the estimators are reached for the minimal values of parameter p . In our case, this corresponds to one single pixel of the echo included in the filtering window (i.e. the corner of the structure). If the number of deterministic pixels increases, the value of the estimators decreases, that justify the shape of the square structures on the images and the decreasing values along the edges and inside the square. From (6) and (7), for low values of p , Skewness can be approximated by $1/\sqrt{p}$ and Kurtosis by $1/p$. This explains that for a 11×11 window, the highest value on the image of Skewness is close to $11 = \sqrt{11 \times 11}$ and $121 = 11 \times 11$ for Kurtosis (Fig. 2).

A critical case exists for the Kurtosis. Indeed, when p goes above 0.5 (there are more deterministic pixels than pixels from the noisy background), the Kurtosis value increases with p (Fig. 3). The case of $p = 1$ is particular (infinite Kurtosis) and is put to its maximum value on the image. For Skewness, negative values appear for $p > 0.5$ (Fig. 2(a) near the center of the square) as predicted by Fig. 3.

In the following, only the results obtained with Kurtosis will be considered, the behaviours of the two estimators being similar for $p < 0.5$.

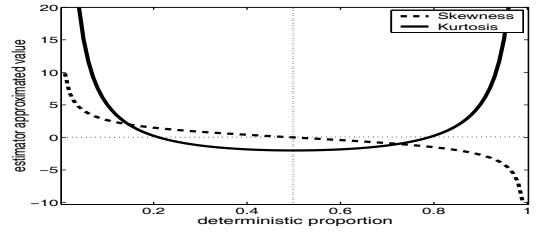


Fig. 3. Approximation of the HOS estimators versus the deterministic pixels proportion p .

2.3. Influence of the size of the computation window

In the previous subsection, the computation window was corresponding to the size of the element to detect, the echo (11×11), allowing to see some properties of the method. The influence of the choice of this size is studied in this subsection.

We can see on Fig. 3 that if $p > 0.5$, Kurtosis increases again to become infinite for $p = 1$ (all pixels of the window correspond to the echo). As a consequence, if we choose a window smaller than the element to detect, the square structure on Kurtosis image does not appear clearly (Fig. 4(a)). A solution is to choose a size avoiding this case: for instance a size twice as big as the echo (Fig. 4(b)). Note that in practice, real echoes are very small. Furthermore, the use of a too small filtering window does not lead to a robust estimation of the HOS.

We have seen in the subsection 2.2 that the highest value of Kurtosis on the image only depends on the size of the computation window and that bigger is this window, higher is this value. But this size has to be restricted. Indeed, we have seen in the same subsection that the size of the square structure on the Kurtosis image is equal to the size of the echo plus the size of the computation window. If several elements have to be detected on the SAS image, the squares associated to each echo can overlap if a too big computation window is used. This situation is illustrated on Fig. 5(b):

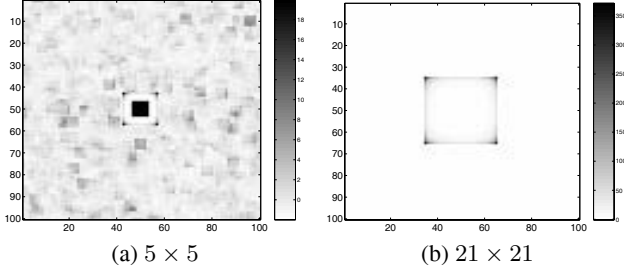


Fig. 4. Kurtosis evaluated on the synthetic image with different sizes of window.

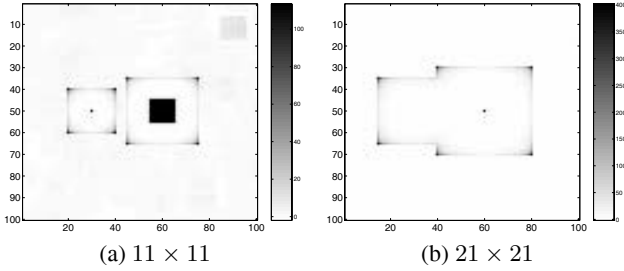


Fig. 5. Kurtosis evaluated on a synthetic image containing two echoes with different sizes of window.

Kurtosis has been evaluated on an other synthetic image with two echoes of different sizes, different amplitudes and distant of 15 pixels. A solution is to choose a size that takes this into account (Fig. 5(a)). On this last figure, we can verify the independence of the Kurtosis value from the amplitude of the echo.

To conclude, we can say that the choice of the size of the window is a tradeoff between the size of the element we have to detect, and the space separating two features.

3. FOCUSING OF THE RESULTS

In this section, the second step of the detection method is described. It consists in focusing the detected squares to one point corresponding to the correct location of the sought element. This is achieved by a simple correlation of the Kurtosis image with a frame with well suited dimension. The size of this frame must be chosen taking into account the size of the window used to build the image, and the dimension of the sought element (the echo), as we have seen in section 2.2. We can see on Fig. 6 the result of a correlation using a 31×31 window on the Kurtosis image of the synthetic image (Fig. 1) obtained with a 21×21 window (Fig. 4(b)). We can see on the zoomed image (Fig. 6(b)) the maximum value of the correlation at the exact position of the center of the echo of the SAS image. A simple threshold of this last image then allows an easy detection and precise location of the object.

Given the size of the window, which is fixed before the Kurtosis image was built, the dimension of the echoes is not accurately known. To take this fact into account, a solution is to take, for the correlation, a frame with a given “thickness”. For example, on the synthetic image containing two echoes used in section 2.3, the size of the echoes were respectively 11×11 and 21×21 . If a 41×41 frame is chosen, only the wider echo is correctly focused (Fig. 7(a)). To solve this problem, a 41×41 (external size) frame with a thickness of 5 is chosen. This allows to have a relatively

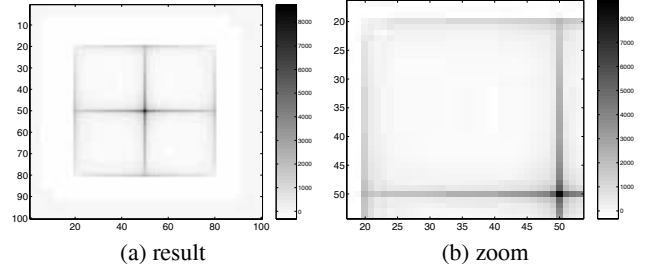


Fig. 6. Correlation of Kurtosis image 21×21 with a 31×31 frame.

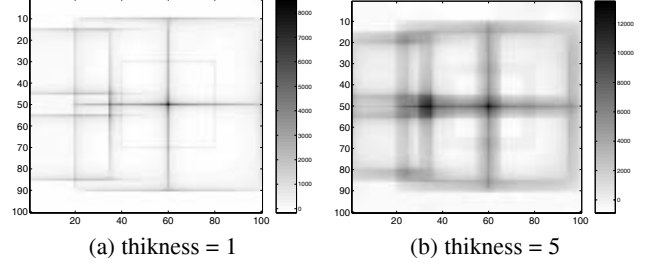


Fig. 7. Correlation of Kurtosis image 21×21 of the synthetic image containing two echoes with a 41×41 frame with different thickness.

good detection of the two echoes (Fig. 7(b)).

4. RESULTS ON REAL DATA

The proposed detection method has been tested on various real SAS data. These data have been provided by the DGA (Délégation Générale pour l’Armement, France).

4.1. SAS data with underwater mines laying on the sea bed

In this subsection, the method is performed on a SAS image containing an underwater mine laying on the sea bed recognizable thanks to the shadow projected on the sea bed and the echoes reflected by the object. This image represents a region of 3.5m by 10m, with a resolution of approximately 1cm in both dimensions (Fig. 8(a)). After the computation of the Kurtosis image using a 21×21 window, taking into account the dimension of the echoes and the space in between, the resulting image is correlated with a 31×31 frame with a 4 pixels thickness (permitting to take into account the uncertainty on the dimension of the echoes). On the result (Fig. 8(b)) we can recognize two main little regions on the left, with high values, corresponding to the two main echoes on the SAS image characterizing the mine.

4.2. SAS data with buried object

In this subsection, the detection method is tested on more complex SAS data. Indeed, the SAS image contains several buried or partially buried objects. This image represents a sea bed region of about 9m by 10m, with a resolution of 6cm in both dimensions. On this image (Fig. 9), the echoes (see the numbered boxes) reflected by the objects are hardly visible apart from a partially buried cylindrical mine on the left (1). After having built the Kurtosis image with a 11×11 computation window, the result is correlated with

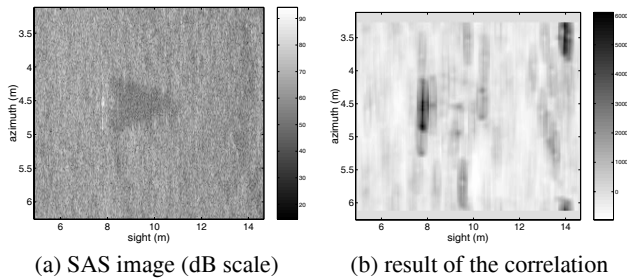


Fig. 8. SAS image containing a laying mine and result obtained by the detection method.

a 17×17 frame with a 4 pixels thickness. The result (Fig. 10) is extremely promising: buried objects, that were badly visible on the SAS image, appear clearly on the resulting image (a rock (2) and a buried mine (3) on the right of the cylindrical mine, an other buried mine at the top (4) and another on the left (5)). Some false alarms appearing at the bottom are due to unidentified objects.

5. CONCLUSION AND PERSPECTIVES

A detection method in SAS imagery, using higher order statistics, has been proposed and studied in this paper. This detection uses the echoes reflected by the objects contained on the scene. The correlation step focuses the result in order to obtain the exact location of the objects. The robustness of the method can be underlined, the result being theoretically independent from the amplitude of the echoes and of high value on the echoes compared with the noise. A drawback of this method could be the fact that we should to know some characteristics of the echoes (maximal dimension, minimal space between them) before using the process, but this can be solved by simple *a priori* knowledge on the sought objects. In the correlation step, the use of a thick frame allows to model the imprecision on the knowledge of the echo dimension. The promising results obtained on real data, even in the case of buried objects with a low signal to noise ratio, highlights the interest of this method.

The perspectives of this work include the recognition and classification of the detected objects. An other idea would be to use the segmentation results provided by other methods [4] to reduce the false alarm rate.

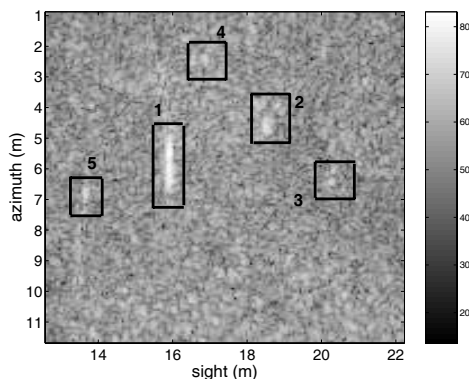


Fig. 9. SAS image containing buried objects (dB scale).

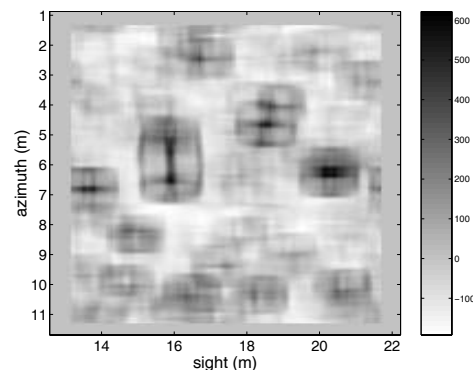


Fig. 10. Result obtained by the detection method.

Note: This work was supported by the French National Defense Department and the French Navy (DGA/DCE/GESMA) under Grant 01-59-918.

6. REFERENCES

- [1] J.T. Broach, R.S. Harmon, and G.J. Dobeck, “conference chair,” in *Proc. of SPIE, Detection and Remediation Technologies for Mines and Minelike Targets VII*, Orlando, Florida, USA, Apr. 2002, vol. 4742.
- [2] J. Chanussot, F. Maussang, and A. Hétet, “Scalar Image Processing Filters for Speckle Reduction on Synthetic Aperture Sonar Images,” in *Proc. of MTS/IEEE Oceans’02 conference*, Biloxi, Mississippi, USA, Oct. 2002, pp. 2294 – 2301.
- [3] M. Mignotte, C. Collet, P. Pérez, and P. Bouthemy, “Unsupervised Markovian Segmentation of Sonar Images,” in *Proc. of ICASSP’97*, Munchen, Germany, May 1997, vol. 4, pp. 2781 – 2785.
- [4] F. Maussang, J. Chanussot, and A. Hétet, “Automated Segmentation of SAS Images using the Mean – Standard Deviation Plane for the Detection of Underwater Mines,” in *Proc. of MTS/IEEE Oceans’03 conference*, San Diego, California, USA, Sept. 2003, pp. 2155 – 2160.
- [5] M.J. Hinich, “Testing for Gaussianity and Linearity of a Stationary Time Series,” *Journal of Time Series Analysis*, vol. 3, no. 3, pp. 169 – 176, 1982.
- [6] J.M. Mendel, “Tutorial on Higher Order Statistics (Spectrum) in Signal Processing and System Theory: the Critical Results and some Applications,” *Proceedings of IEEE*, vol. 79, no. 3, pp. 278 – 305, Mar. 1991.
- [7] T. Aridgides, M. Fernández, and G. Dobeck, “Side Scan Sonar Imagery Fusion for Sea Mine Detection and Classification in Very Shallow Water,” in *Proc. of SPIE, Detection and Remediation Technologies for Mines and Minelike Targets VI*, Orlando, Florida, USA, Apr. 2001, vol. 4394, pp. 1123 – 1134.
- [8] M.G. Kendall and A. Stuart, *The Advanced Theory of Statistics*, vol. 1, Charles Griffin & Company Limited, London, United Kingdom, 2nd edition, 1963.